Biosensors and Bioelectronics 47 (2013) 99–105

Contents lists available at SciVerse ScienceDirect

Biosensors and Bioelectronics

journal homepage: www.elsevier.com/locate/bios

High-κ $GdTi_xO_y$ sensing membrane-based electrolyte–insulator–semiconductor with magnetic nanoparticles as enzyme carriers for protein contamination-free glucose biosensing

Min-Hsien Wu [a,1], Hung-Wei Yang [b,1], Mu-Yi Hua [b,1], Yen-Bo Peng [c], Tung-Ming Pan [c,*]

[a] Graduate Institute of Biochemical and Biomedical Engineering, Chang Gung University, Kwei-Shan, Tao-Yuan 33302, Taiwan
[b] Department of Chemical and Materials Engineering, Chang Gung University, Kwei-Shan, Tao-Yuan 33302, Taiwan
[c] Department of Electronics Engineering, Chang Gung University, Kwei-Shan, Tao-Yuan 33302, Taiwan

ARTICLE INFO

Article history:
Received 2 December 2012
Received in revised form
19 February 2013
Accepted 8 March 2013
Available online 20 March 2013

Keywords:
Electrolyte–insulator–semiconductor (EIS)
$GdTi_xO_y$
Glucose
Fe_3O_4
Magnetic nanoparticles (MNPs)

ABSTRACT

This paper reports an electrolyte–insulator–semiconductor (EIS) device featuring a novel high-κ $GdTi_xO_y$ sensing membrane for high-performance pH sensing and glucose biosensing. The effect of the annealing temperature (700, 800, or 900 °C) on the sensing properties of the $GdTi_xO_y$ membranes was investigated. The $GdTi_xO_y$ EIS device annealed at 900 °C exhibited the greatest pH sensing performance, including the highest sensitivity (62.12 mV/pH), the smallest hysteresis voltage (5 mV), and the lowest drift rate (0.4 mV/h), presumably because of its well-crystallized $GdTi_xO_y$ structure. To overcome the problems typically encountered during the practical application of biosensors (e.g., protein adsorption; preservation of enzymatic activity), we employed Fe_3O_4-based magnetic nanoparticles (MNPs) as enzyme carriers. The adsorption of serum protein on the unmodified sensing membrane led to poor EIS-based pH sensing ($r^2=0.71$); the performance was greatly improved, however, after attaching the MNPs to the sensing membrane, thereby blocking protein adsorption significantly (by 98%) and allowing excellent pH sensing ($r^2=0.99$). Moreover, we prepared a hybrid configuration of the proposed $GdTi_xO_y$ membrane-EIS, with magnetically attached glucose oxidase-immobilized MNPs, for glucose biosensing. The use of MNPs as enzyme carriers effectively preserved the enzymatic activity of glucose oxidase, with 45.3% of the original enzymatic activity retained after 120 h of storage at 4 °C (compared with complete loss of the free enzyme's activity under the same storage conditions). In addition, the proposed biosensor exhibited superior detection sensitivity of 11.03 mV/mM relative to that (8.17 mV/mM) obtained using the conventional enzyme immobilization method. Finally, we established the accuracy of the proposed method for blood glucose measurement; gratifyingly, blood glucose detection was comparable with the high-sensitivity glucose quantification obtained using a commercial glucose assay kit.

1. Introduction

Electrolyte–insulator–semiconductor (EIS) systems and ion-sensitive field-effect transistors (ISFETs) are solid state electronic devices that allow chemical sensing of ionic concentrations (e.g., H^+ ions for pH measurement) in solution (Schoning and Poghossian, 2006). Compared with ISFET-based sensing devices, the key advantages of EIS-based sensors are their simpler structures and fabrication processes. An EIS features a four-component structure, encompassing a reference electrode, an electrolyte, an insulator sensing membrane, and a semiconductor layer. Rare earth (RE) element oxides (e.g., Y_2O_3 Pan and Liao (2007), Pr_2O_3 Pan and Liao (2008), Er_2O_3 Pan et al. (2009a), Tm_2O_3 (Pan et al., 2009b) appear to be promising substitutes for silicon nitride, due to their high dielectric constants (high-κ), large conduction band offsets, and good thermal stability in the presence of a silicon substrate. Nevertheless, the technical problems of using an RE oxide as the insulator sensing membrane are silicate formation and high hygroscopicity (Jeon and Hwang, 2003), which both affect the sensing performance. These technical hurdles can be overcome through the incorporation of TiO_2 or Ti in the high-κ RE oxide membrane, resulting in lower reactivity toward water, thinner interfacial layers, higher capacitance, and lower leakage currents characteristics (van Dover, 1999; Jeon and Hwang, 2002) that are valuable when exploiting EIS-based sensing devices for the detection of ions or molecules in aqueous solutions. In addition to the aforementioned RE oxide materials, gadolinium oxide (Gd_2O_3) is another potential material for fabricating the sensing membrane in an EIS; it features an appropriate lattice

* Corresponding author. Tel.: +886 3 211 8800x3349; fax: +886 3 211 8507.
E-mail address: tmpan@mail.cgu.edu.tw (T.-M. Pan).
[1] M.-H. Wu, H.-W. Yang, and M.-Y. Hua contributed equally to this work.

0956-5663/$ - see front matter © 2013 Elsevier B.V. All rights reserved.
http://dx.doi.org/10.1016/j.bios.2013.03.013

compatible with silicon, good thermal stability in the presence of silicon, and large conduction and valence band offsets (Fanciulli and Scarel, 2007). Nevertheless, to the best of our knowledge, there are relatively few studies on the properties of $GdTi_xO_y$ sensing membranes (prepared through incorporation of TiO_2 in Gd_2O_3) and their performance in resulting EIS-based pH sensors, except our previous reports (Her et al., 2013; Pan et al., 2013).

Magnetic nanoparticles (MNPs), generally consisting of such magnetic materials as iron, cobalt, and nickel, are a class of nanoparticles that can be manipulated under a magnetic field. MNPs have been actively exploited in a wide range of fields, including magnetic resonance imaging (Veiseh et al., 2010), targeted drug delivery (Rahimi et al., 2010; Yang et al., 2012), virus detection (Perez et al., 2003), gene therapy (Hood et al., 2002), radiotherapy (Hafeli et al., 1995), bio-separation (Lewin et al., 2000), and catalysis (Hong et al., 2008). Notably, the performance of MNP-based bio-separation or catalytic processes can be improved greatly as a result of the higher surface area–to–volume (SAV) ratio of the MNPs (Katz et al., 2004), allowing, for example, more biomolecules on the MNPs to react with the targeted substrate. Taking advantage of the characteristic nanoscale dimensions and high SAV ratios of MNPs, as well as their ability to be manipulated under a magnetic field, we employed Fe_3O_4-based MNPs as enzyme carriers for EIS-based biosensing. Our approach was predicated upon the enzyme-linked MNPs being attracted magnetically to the sensing membrane of the EIS for biosensing, but subsequently discarded after use simply by releasing the magnetic field while preserving the EIS located underneath. The use of enzyme-linked MNPs not only enhances enzymatic catalysis–and, thereby, improve detection sensitivity–but also prevents the adsorption of co-existing substances (e.g., proteins) from the tested sample. In this study, we investigated the sensing properties of $GdTi_xO_y$ sensing membranes fabricated on silicon substrates through reactive radio frequency (rf) sputtering with subsequent rapid thermal annealing (RTA) treatment at 700, 800, or 900 °C. Furthermore, we discussed the effect of annealing temperature on the sensing characterictics in terms of detection sensitivity, hysteresis, and signal drifting. We also investigated the influence of the adsorption of co-existing substances (e.g., serum proteins) from the tested sample on the performance of the EIS-based pH sensor. Furthermore, we used XPS analysis to examine the role of the MNPs as protectors of the sensing membrane from contamination by serum proteins. To demonstrate the feasibility of using enzyme-linked MNPs on an EIS-based biosensor, we investigated such systems for glucose biosensing. Finally, we found that the accuracy of our proposed method for blood glucose measurement was comparable with that of the high sensitivity obtained using a commercial glucose assay kit.

2. Materials and methods

2.1. Fabrication of EIS-based pH sensor

The EIS structure with a high-κ $GdTi_xO_y$ sensing membrane was fabricated on a 4-in. p-type (100) silicon wafer. Prior to deposition of the $GdTi_xO_y$ sensing membrane, the wafer was cleaned using a standard Radio Corporation of America (RCA) process. A film (~40 nm) of $GdTi_xO_y$ was then deposited on the silicon substrate through reactive rf sputtering using gadolinium (Gd) and titanium (Ti) as targets in a diluted O_2 ambient ($Ar/O_2 = 5$ sccm/2 sccm) at a substrate temperature of 27 °C. All of the samples were then annealed at different temperatures (700, 800, 900 °C) under ambient O_2 conditions for 30 s using a lamp-based RTA system. An aluminum (Al) film (400 nm) was subsequently deposited onto the reverse side of the wafer, acting as a backside contact, through a thermal evaporation method. The sensing zone on the deposited $GdTi_xO_y$ membrane was then defined by a standard photolithography process using SU8-2005 (MicroChem, USA) as a photoresist, followed by assembly of the prepared EIS structures on the copper (Cu) line of a custom-made printed circuit board (PCB), using a silver gel to form the conductive line. A hand-made epoxy package was used to encapsulate the EIS structure from the Cu line.

2.2. Using MNPs to prevent serum protein adsorption and the effect of protein adsorption on EIS-based pH sensing

The high-magnetization Fe_3O_4 MNPs were synthesized based on a previously reported procedure (Yang et al., 2012). MNP suspensions (10 μL; 10, 15, or 20 mg/mL) were prepared by suspending the MNPs in deionized (DI) water. The suspensions were then placed onto the surfaces of fabricated $GdTi_xO_y$ sensing membranes under an applied magnetic field to immobilize the MNPs. The prepared sensing membranes with and without attached MNPs were subsequently immersed in fetal bovine serum (FBS) suspension (unless otherwise stated, all chemicals were purchased from Sigma, Taiwan) for up to 12 h. After immersion, the magnetic field was turned off, and the sensing membranes were washed with DI water twice to remove the attached MNPs. The treated sensing membranes were then analyzed through a surface survey using high-resolution XPS (ULVAC-PHI Quantera 2000). In this study, the nitrogen peak intensity in the XPS spectra was used to quantify the serum proteins adsorbed on the sensing membranes (Boxshall et al., 2006). To determine the impact of serum protein adsorption on EIS-based sensing, pH sensing was performed with the $GdTi_xO_y$ sensing membranes in both the presence and absence of the protecting MNPs, using the same procedure described above.

2.3. Preparation of MNP-GOx complexes

The enzyme-linked MNPs were prepared using a previously reported procedure [Yang et al., 2012]. Briefly, 1-ethyl-3-[3-dimethylaminopropyl]carbodiimide hydrochloride (EDC-HCl, 24 mg) and *N*-hydroxysulfosuccinimide (sulfo-NHS, 27 mg) were dissolved in 0.5 M 2-morpholinoethanesulfonic acid (MES, 2 mL) in the dark. An aliquot (0.2 mL) of this solution was mixed with the solution of the MNPs (10 mg/mL, 0.2 mL) at 25 °C, followed by vortexing for 30 min in the dark. After separation, the MNPs were washed with 0.1 M MES buffer (0.8 mL) and resuspended in MES (0.2 mL). The treated MNPs were then mixed with solutions of glucose oxidase (GOx; from Jack Beans; ~100 U/mg; 0.1 mL) at various concentrations (0.2–30 mg/mL) by vortexing at 25 °C for 2 h. The GOx-linked MNPs were subsequently washed with DI water to remove any unbound GOx and finally dispersed in DI water (0.2 mL). Each glucose oxidase–coupled MNPs (MNP-GOx) complex comprised an MNP core (Fig. 1: gray color) presenting carboxyl linkers (Fig. 1: green color), which interacted with the GOx units (Fig. 1: blue color); the mean diameter of the MNP-GOx complexes was approximately 18.9 nm, as measured using transmission electron microscopy (TEM). The amount of GOx immobilized on the MNPs was quantified optically using a spectrometer (Lambda 800/900, PerkinElmer, USA) at a set wavelength of 277 nm.

2.4. Enzymatic activity of GOx immobilized on MNPs

GOx catalyzes the oxidation of glucose to hydrogen peroxide (H_2O_2), and D-gluconolactone. The enzymatic activity of free GOx and of the enzyme immobilized on MNPs (MNP-GOx) were, therefore, analyzed through the production of H_2O_2 [Hua et al., 2012].

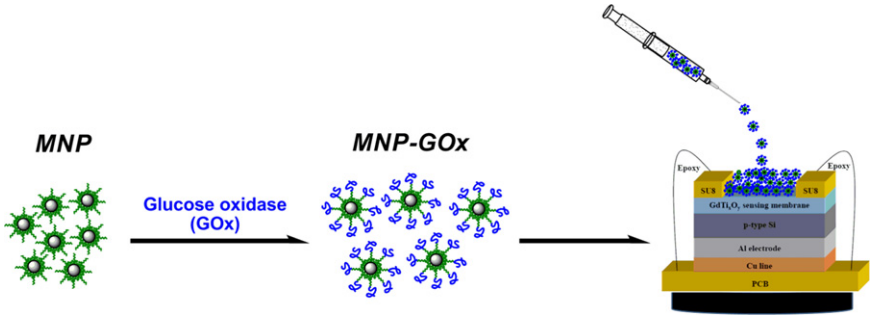

Fig. 1. Schematic representation of the preparation of an EIS glucose biosensor featuring magnetically attached GOx-MNPs.

The generation of H_2O_2 was quantified colorimetrically using a commercial H_2O_2 assay kit (BioVision, USA). Briefly, the GOx and MNP-GOx were thoroughly mixed, respectively, with 10 mM glucose solution (1 mL) under O_2-saturated conditions for 1 min. Next, an aliquot (50 μL) of the supernatant was mixed with the H_2O_2 assay kit reagent (50 μL), based on the manufacturer's instructions. After incubation for 30 min at room temperature, the optical adsorption at 570 nm was measured using a spectrometer. The amount of H_2O_2 produced was then quantified through a H_2O_2 standard curve. The relative activity is defined herein as the percentage of H_2O_2 production catalyzed by the free GOx or MNP-GOx relative to that catalyzed by free fresh GOx. To study the effects of the storage temperature and time on the enzymatic activity, GOx and the MNP-GOx suspension were kept at 4 or 25 °C for up to 120 h, with the relative activity evaluated every 12 h.

2.5. MNP-GOx/GdTi$_x$O$_y$ versus GOx-encapsulating alginate gel/GdTi$_x$O$_y$ EIS-based glucose sensing

To evaluate the performance of the MNP-GOx/GdTi$_x$O$_y$ EIS-based biosensor, glucose sensing was performed and compared with that based on a conventional enzyme immobilization method (hydrogel-based enzyme encapsulation). Briefly, a solution of MNP-GOx (20 mg/mL, 10 μL), prepared as previously described, was drop-deposited onto the GdTi$_x$O$_y$ sensing membrane of the EIS sensor and were magnetically immobilized, as shown in Fig. 1. To prepare the GOx-encapsulated alginate gel/GdTi$_x$O$_y$ EIS-based glucose sensor, a solution of GOx in phosphate-buffered saline (1X PBS) was thoroughly mixed with a 1% (w/v) alginate suspension to form a suspension featuring a final GOx concentration of 0.1 mg/L. This suspension was loaded onto a clean glass slide and covered with another glass slide with a 1-mm-thick spacer in between, thereby defining the thickness of the enzyme-encapsulated alginate thin gel. In the gelatinization process, the sandwich-like structure was incubated in 102 mM calcium chloride ($CaCl_2$) solution for 10 min. The alginate thin gel was then shaped according to the sensing zone of the EIS device and subsequently attached onto the surface of the GdTi$_x$O$_y$ sensing membrane [Wu et al., 2010]. For glucose biosensing, glucose standard solutions with concentrations ranging from 0.5 to 6 mM were prepared by dissolving glucose power in 1X PBS. The pH of the prepared glucose standard solutions was then examined using a pH meter to ensure that all of the standards were identical. In the biosensing operation, the EIS sensors with either MNP-GOx magnetically immobilized or an enzyme-encapsulating alginate thin gel attached were immersed in the glucose standard solutions for 10 min. The *C–V* plots were then recorded as mentioned above. The EIS sensors with the immobilized enzyme were rinsed with RO water after each detection event.

2.6. Evaluation of MNP-GOx/GdTi$_x$O$_y$ EIS-based Blood glucose detection

A blood sample was first diluted twofold in PBS and then measured using the glucose detection methods described above. To ensure the accuracy of biosensing, the glucose concentration of the diluted blood sample was also examined using a commercial glucose assay kit (BC-0019, MeDiPro, Taiwan). The experimental procedures were based on the manufacturer's instructions.

3. Results and discussion

3.1. Performance of GdTi$_x$O$_y$ membrane–based EIS pH sensors

To evaluate the pH sensing performance of our GdTi$_x$O$_y$ membrane-based EIS sensors, we examined their behavior toward standard buffer solutions having values of pH ranging from 2 to 12. In the capacitance–voltage (*C–V*) curves for the standard buffer solutions (Fig. 2A), we observe pH-dependence for the EIS pH sensor incorporating the GdTi$_x$O$_y$ membrane annealed at 900 °C. This EIS-based pH sensor provided distorted *C–V* curves, as has been reported in the literature [Wu et al., 2010], presumably attributable to the presence of interfacial traps in the oxide. In EIS-based pH sensing, more importantly, a change in pH normally leads to a flat-band voltage shift of the *C–V* curves, mainly due to ionization of the surface OH groups by H^+ or OH^- ions [Fung et al., 1986], in turn modifying the surface potential through dipole formation on the sensing membrane. The inset to Fig. 2A displays the reference voltage of the GdTi$_x$O$_y$ sensing membrane annealed at 900 °C as a function of pH. Here, the reference voltages were determined from the obtained *C–V* curves at a normalized capacitance of 0.5 (Wu et al., 2011; Her et al., 2013). This EIS-based pH sensor exhibited a linear response upon increasing the pH from 2 to 12, with an evaluated detection sensitivity of 62.12 mV/pH. To determine the pH detection sensitivities of the GdTi$_x$O$_y$ membranes that had been subjected to various annealing temperatures, we recorded their *C–V* curves and then evaluated them based on the approach described above. Fig. 2B reveals that the EIS device featuring the membrane annealed at 900 °C exhibited the best pH detection sensitivity (62.12 mV/pH) within the studied experimental conditions, presumably because this annealing temperature led to the formation of a well-crystallized $Gd_2Ti_2O_7$ structure (Her et al., 2013). As a whole, the GdTi$_x$O$_y$ membranes explored in this study demonstrated pH detection sensitivity superior to those of materials commonly used for ISFET- and EIS-based sensing, namely Si_3N_4 (46–56 mV/pH) (Matsuo et al., 1979), Al_2O_3 (52–58 mV/pH) (Matsuo et al., 1979; Miao et al., 2003), Ta_2O_5 (56–58 mV/pH) (Poghossian and Schoning, 2004), ZnO_2 (58 mV/pH) (Liao et al., 2007), and Nd_2TiO_5 (50–57 mV/pH) (Pan et al., 2009c). In addition to detection sensitivity, hysteresis and signal drifting

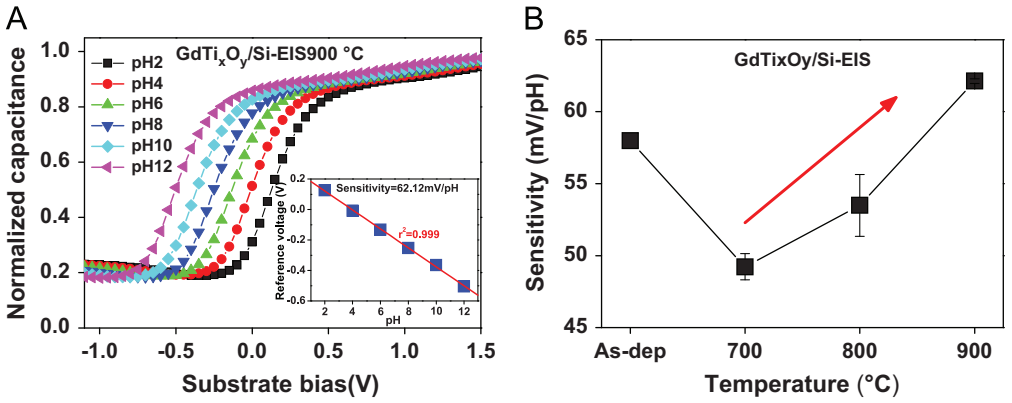

Fig. 2. (A) *C–V* curves of the EIS sensor incorporating the GdTixOy sensing membrane annealed at 900 °C, recorded at various values of pH (pH 2–12). Inset: Reference voltage of the EIS sensor (900 °C) at various values of pH (pH 2–12). (B) The pH detection sensitivities of the EIS sensors incorporating GdTixOy sensing membranes annealed at 700, 800, and 900 °C. Data are expressed as means ± standard deviation (n=3).

are two other critical performance features affecting the success of a sensing device. In this study, we evaluated the hysteresis effects of EIS devices featuring different $GdTi_xO_y$ sensing membranes through direct immersion of the prepared sensors in each pH standard solution for up to 1500 s in a set cycle of pH 7→4→7→10→7 (Fig. S1A in supplementary material). The EIS device incorporating the $GdTi_xO_y$ membrane annealed at 900 °C had a lower hysteresis voltage (~5 mV) than those prepared at the other annealing temperatures. In addition, we evaluated the signal drift of the pH sensing by measuring the change in the reference voltage. The EIS device incorporating the membrane annealed at 900 °C exhibited the best long-term stability (slope=0.4 mV/h) in comparison with the other annealing temperatures (Fig. S1B in supplementary material).

3.2. Using MNPs as enzyme carriers for EIS-based biosensing

The use of enzymes as biological recognition elements can extend the applications of EIS-based pH sensing devices to highly selective biosensing. Biosensors of these kinds are virtually all configured by integrating a pH-EIS mechanism with an enzyme-immobilizing element. In the real application of a biosensor, however, repeated operations might lead to contamination, in turn affecting the biochemical conditions (e.g., pH, enzyme activity) in the enzyme-immobilizing element. The inconsistency of such a bio-recognition element might result in bias between run-to-run detection events. In addition, the adsorption of other species in the tested sample (e.g., serum proteins in blood samples) onto the transducer (e.g., EIS device) might change its properties, thereby leading to detection bias. Overall, these two technical issues make it necessary to calibrate the system for each detection event. Moreover, the success of a biosensor relies on its working lifetime, with preservation of the biological recognition element being the key technical hurdle. Biomolecules are generally delicate and, thereby, difficult to preserve in terms of function and activity, unless an effective approach is adopted to stabilize them, in the biological recognition elements of biosensors. Taken together, all of these problems can be solved simply by using a fresh biological recognition element for each biosensing task. We have previously proved that EIS-based pH sensors based on TiO_2-incorporated RE oxides have long-term stability (at least 140 days) (Wu et al., 2010). Therefore, we suspected that such EIS-based biosensing devices might become more practical if the biological recognition element were disposable. In this study, we tested the use of MNPs as enzyme carriers to (i) prevent the adsorption of interfering substances from the tested sample, (ii) ensure that the biological recognition element would be disposable, and (iii) enhance the sensitivity of biosensing as a result of a high SAV ratio.

We performed a series of experiments to confirm the advantageous features of MNPs as enzyme carriers in EIS-based biosensing. First, we explored the ability of the MNPs to prevent serum protein adsorption on the sensing membrane of the EIS device. Briefly, we deposited MNP suspensions with different concentrations (10, 15, and 20 mg/mL) and then immobilized the MNPs onto the surface of the $GdTi_xO_y$ sensing membrane under a given magnetic field. The prepared sensing membranes, with and without attached MNPs, were subsequently immersed in FBS suspension; the adsorbed proteins were quantified through XPS analysis using the intensity of the nitrogen peak as an index (Boxshall et al., 2006). Fig. 3A–D present the obtained XPS spectra of the sensing membranes treated with MNP suspensions at 0 (control), 10, 15, and 20 mg/mL. The magnitude of the nitrogen (N) peaks decreased upon increasing the MNP concentration. After normalizing the intensity of the nitrogen peak to that of the control sample, Fig. 4A reveals the quantitative relationship between the percentage of protein adsorption and the MNP concentration. The attachment of MNPs to the surface of the sensing membrane decreased serum protein adsorption significantly–by 53, 73, and 98% for MNP concentrations of 10, 15, and 20 mg/mL, respectively–relative to that of the control sample. In this study, the diameter of the MNPs was 15 nm, comparable with the general size of protein molecules. As a result, the attached MNPs on the surface of the sensing membrane could physically hinder the adsorption of serum protein. Moreover, Fig. 4A reveals that the MNP suspension having the highest tested concentration (20 mg/mL) was more effective at protecting against serum protein adsorption, presumably because of a greater coverage of MNPs on the surface of the sensing membrane or a thicker MPN layer. To realize the extent to which the EIS-based sensing was affected by the serum protein adsorption, we performed pH sensing using the previous sensing membranes treated with MNP suspensions at 0 (control) and 20 mg/mL. Fig. 4B reveals that the adsorption of serum protein on the $Gd_2Ti_2O_7$ sensing membrane led to poor sensing performance (correlation coefficient: r^2=0.71), but it was greatly improved by the anti-protein adsorption effect of MNPs, which blocked serum protein adsorption significantly (by 98%; Fig. 4A) and, therefore, resulted in excellent pH sensing (r^2=0.99). The EIS-based pH sensing mechanism was described well by a site-binding model (Fung et al. 1986). Briefly, the reference voltage of an EIS is directly proportional to its surface potential, which is dependent on the nature of the sensing membrane (e.g., the pH of the electrolyte, the double layer capacitance, or the total number of surface sites available for interacting with ions). A possible explanation of the

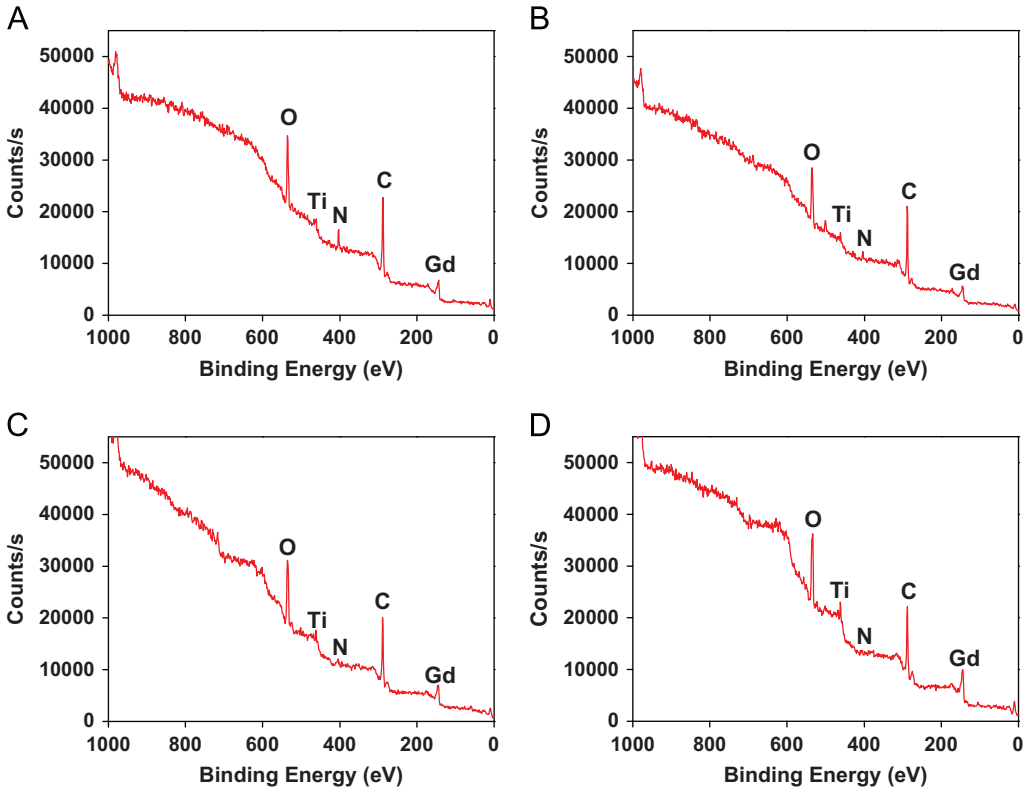

Fig. 3. XPS surface survey spectra of GdTi*x*O*y* sensing membranes with different concentrations [(A) 0 mg/mL (control), (B) 10 mg/mL, (C) 15 mg/mL, and (D) 20 mg/mL] of MNPs attached in fetal

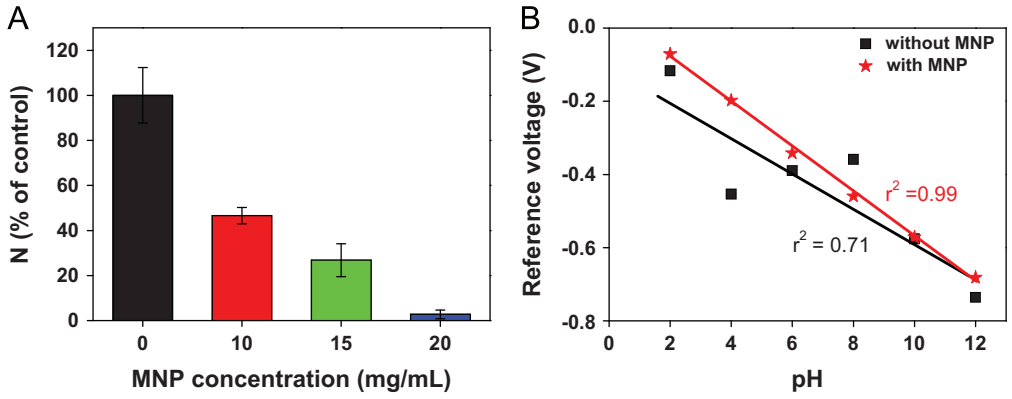

Fig. 4. (A) Quantification of nitrogen (N) atoms on the surfaces of these MNP-treated sensing membranes after normalizing the intensity of the signals for the N atoms in the spectra relative to that of the control sample. Data are expressed as means ± standard deviation (n=3). (B) Comparison of pH sensing performance of EIS sensors incorporating sensing membranes prepared in the presence or absence of MNPs (20 mg/mL).

results in Fig. 4B is that the adsorption of serum protein blocked the surface sites that would have reacted with ions, or that it altered the double-layer capacitance on the membrane; either way, it would alter the sensing performance of the EIS sensor.

3.3. *Using MNP–glucose oxidase complexes for EIS-based glucose biosensing*

The enzymatic activity of the GOx molecules immobilized on the MNPs played an important role affecting the detection sensitivity of the EIS-based glucose biosensor. In this study, we covalently linked the GOx molecules to the carboxyl groups on the surfaces of the MNPs. To measure the resultant enzymatic activity and to determine the effect of the storage conditions (e.g., temperature, time) on the enzymatic activity, we performed a series of experiments. Fig. 5A reveals the change over time in the relative activities of free GOx and MNP-GOx stored at 4 °C. Not surprisingly, the enzymatic activity of the freshly prepared MNP-GOx was 76.7% of that of the free GOx (at 0 h), due primarily to the effects of steric hindrance and the limited freedom of the GOx molecules on the MNPs [Dessouki and Atia, 2002]. Upon increasing the storage time, however, the decrease in the relative activity of the free GOx was more dramatic than that of the MNP-GOx complex, indicating that immobilization of GOx on the MNPs increased the enzyme's stability and, thus, the working lifetime of the system. We attribute this phenomenon to the denaturation and, thereby, conformational changes of the free GOx under the storage conditions. Conversely, the immobilization of GOx on the carrier appeared to restrict the freedom of the biomolecules to undergo drastic conformational changes; this phenomenon

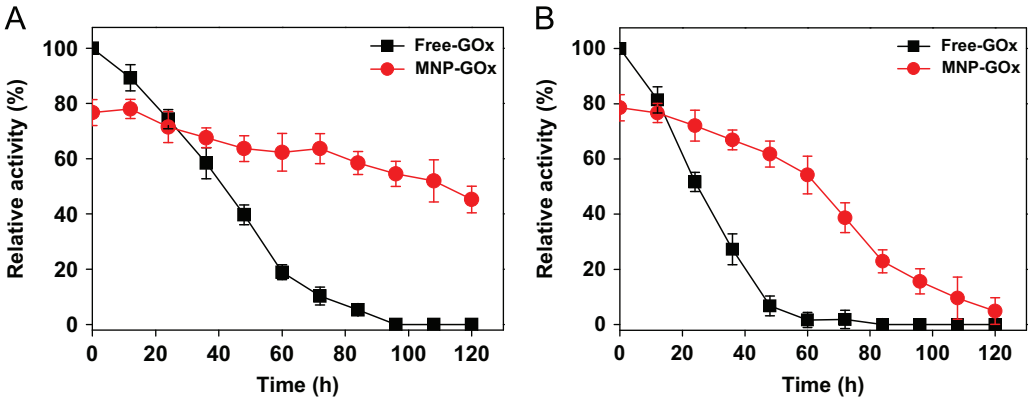

Fig. 5. Temporal variations of the relative activities of free GOx and MNP-GOx stored at (A) 4 and (B) 25 °C. The relative enzymatic activity is defined as the percentage of H2O2 production catalyzed by the free GOx or MNP-GOx complexes relative to that catalyzed by free fresh GOx at 0 h. Data are expressed as means ± standard deviation (n=6).

accordingly decreased the degree of denaturation of the enzyme molecules, thereby contributing to their higher enzyme activity (Dessouki and Atia, 2002). In this study, the free GOx lost it enzymatic activity after storage for 96 h, whereas the MNP-GOx complexes maintained a relative activity of 45.3% after 120 h. Fig. 5B displays the changes over time in the relative activities of the free GOx and the MNP-GOx complexes stored at 25 °C; the variation patterns are similar to those in Fig. 5A. The free GOx lost its enzymatic activity after 60 h of storage, whereas the MNP-GOx complexes maintained a relative activity of 58.4% at that point. Indeed, it took approximately 120 h for the MNP-GOx complexes to lose their enzymatic activity completely. Taken together, it appears that a storage temperature of 4 °C was better than one of 25 °C in terms of preserving the enzymatic activity of GOx in either its free or immobilized states. In addition, the immobilization of GOx on the MNPs significantly enhanced the enzyme's stability—a valuable feature that would improve the working lifetime of a biosensor.

As a demonstration of using MNPs as enzyme carriers for EIS-based biosensing, we tested the system as a glucose sensor. Briefly, MNP-GOx complexes (20 mg/mL, 10 μL), which we had found to have an excellent anti-serum protein adsorption effect, were magnetically immobilized on the $GdTi_xO_y$ sensing membrane (annealing temperature: 900 °C) of the EIS sensor. The prepared EIS sensors were then immersed in glucose standard solutions with concentrations ranging from 0.5 to 6 mM (i.e., covering the physiological blood glucose concentrations of the human body). Fig. 6A reveals that the MNP-GOx EIS sensor exhibited a linear response (r^2=0.99) toward the glucose concentrations in the range from 0.5 to 6 mM, with an evaluated detection sensitivity of 11.03 mV/mM. In this study, we also evaluated the glucose sensing performance of a conventional GOx-encapsulating alginate gel/$GdTi_xO_y$ EIS-based glucose sensor, for comparison with the proposed method. Fig. 6B reveals that glucose sensing based on the conventional enzyme immobilization (gel entrapment) method (r^2=0.96; detection sensitivity: 8.17 mV/mM) was inferior to that of our newly developed system. The most plausible reason for this behavior is the higher SAV ratio of the MNP-GOx complexes over that of the GOx-encapsulating alginate gel, thereby contributing to the higher detection sensitivity of the former. Compared with the published EIS- or ISFET-based glucose biosensors that operate based on conventional enzyme immobilization schemes (detection sensitivity: 6.5–7.7 mV/mM) (Lin et al., 2011; Pan et al., 2010a; Pan et al., 2010b), the proposed MNP-GOx EIS sensor displayed superior sensing performance (detection sensitivity: 11.03 mV/mM). To demonstrate the feasibility of using the proposed sensor for clinical applications, we applied it to detect glucose in three different blood samples. To evaluate the detection accuracy, we compared our results with those obtained through high-sensitivity glucose measurement using a commercial glucose assay kit. Fig. 6C reveals that the results of glucose detection based on the two methods were comparable, indicating that the proposed sensor is as accurate as the commercial method for glucose detection.

4. Conclusions

We have developed an EIS sensor featuring a high-κ $GdTi_xO_y$ sensing membrane deposited on silicon substrate through reactive sputtering and thermal annealing treatment for high-performance pH sensing. Initially, we investigated the effect of thermal annealing on the pH sensing characteristics of the $GdTi_xO_y$ EIS sensors. The EIS sensor incorporating the sensing membrane fabricated with annealing at 900 °C exhibited the optimal pH sensing performance, as evidenced by its high sensitivity (62.12 mV/pH), small hysteresis voltage (5 mV), and low drift rate (0.4 mV/h). We attribute this high performance to the formation of a well-crystallized $GdTi_xO_y$ structure at that temperature. To tackle the problems (e.g., protein adsorption; preservation and control of enzyme activity) normally encountered in the practical use of biosensors, in this study we employed MNPs as enzyme carriers. Taking advantage of their small dimensions, high SAV ratios, and manipulable properties under a magnetic field, the application of enzyme-coupled MNPs as biological recognition elements in biosensors holds great promise (i) to prevent the unwanted adsorption of substances present in the tested sample onto the sensor, (ii) to readily prepare disposable biological recognition elements, and (iii) to enhance the sensitivity of biosensing. Accordingly, our experimental investigations revealed that the adsorption of serum protein on the sensing membrane led to poor EIS-based pH sensing (r^2=0.71), which improved greatly after the attachment of MNPs to the sensing membrane, thereby significantly blocking protein adsorption (by 98%) and leading to excellent pH sensing (r^2=0.99). In addition, we have demonstrated that the use of MNPs as enzyme carriers effectively preserved the enzymatic activity of GOx, with 45.3% of the original enzymatic activity retained after 120 h storage at 4 °C, compared with complete loss for the free enzyme under the same storage conditions. Moreover, the detection sensitivity of our proposed $GdTi_xO_y$ membrane-EIS with magnetically attached GOx-immobilized MNPs (11.03 mV/mM) was better than that (8.17 mV/mM) obtained when using a conventional enzyme immobilization method. Finally, we proved the accuracy of this proposed method for blood glucose measurement, obtaining a level of blood glucose detection that was comparable with the high-sensitivity of glucose quantification measured using a commercial glucose assay kit.

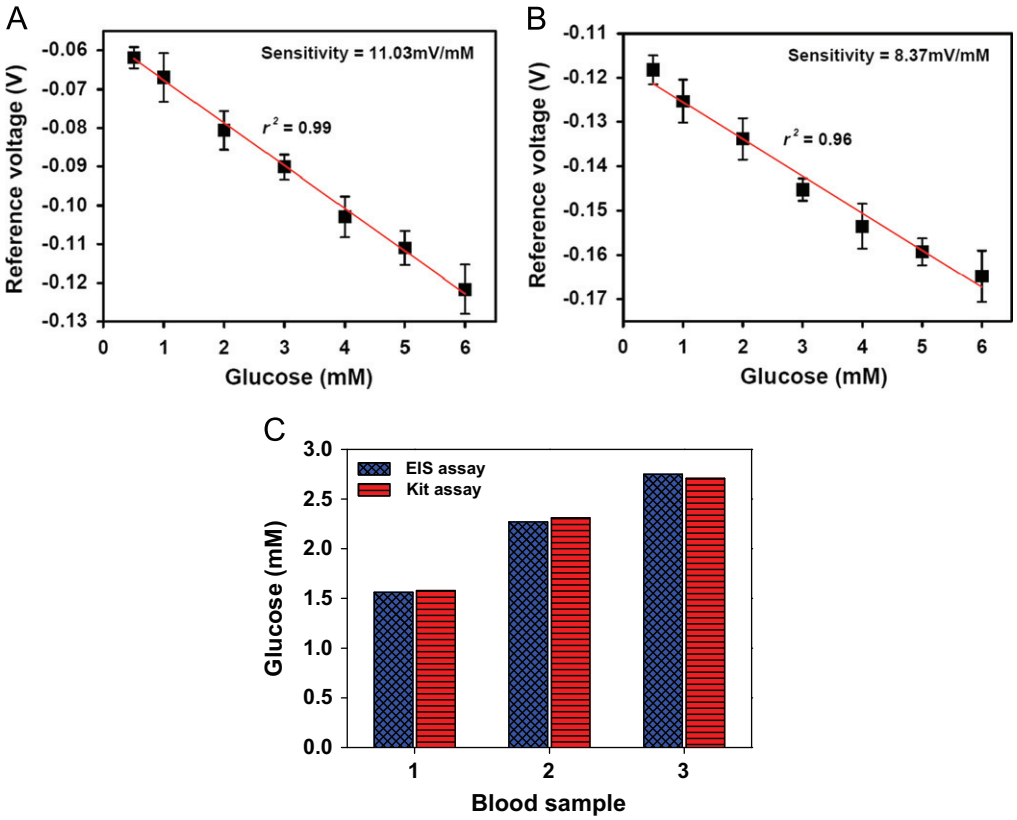

Fig. 6. (A, B) Comparison of glucose biosensing (concentration range: 0.5–6 mM) of the EIS sensor relative to other immobilized-enzyme methods: (A) proposed MNP-GOx. (B) Conventional GOx-encapsulated alginate gel film. Data are expressed as means ± standard deviation (n=6). (C) Accuracy of blood glucose biosensing using the proposed MNP-GOx/GdTi*x*O*y* membrane-based EIS sensor, compared with that obtained using a commercial glucose assay kit. Blood glucose was detected from three individual blood samples.

Acknowledgment

This study was supported by the National Science Council, Taiwan, Republic of China, under contracts NSC-98–2111-E-182-056-MY3, NSC-100–2221-E-182-005, and CMRPD2A0061.

Appendix A. Supporting information

Supplementary data associated with this article can be found in the online version at http://dx.doi.org/10.1016/j.bios.2013.03.013.

References

Boxshall, K., Wu, M.H., Cui, Z., Cui, Z.F., Watts, J.F., Baker, M.A., 2006. Surf. Inter. Anal. 38, 198–201.
Dessouki, A.M., Atia, K.S., 2002. Biomacromolecules 3, 432–437.
Fanciulli, M., Scarel, G., 2007. Rare Earth Oxide Thin Film: Growth, Characterization, and Applications. Springer, Berlin.
Fung, C.D., Cheung, P.W., Ko, W.H.A., 1986. IEEE Transactions on Electron Devices 33, 8–18.
Hafeli, U.O., Sweeney, S.M., Beresford, B.A., Humm, J.L., Macklis, R.M., 1995. Nuclear Medicine and Biology 22, 147–155.
Her, J.L., Wu, M.H., Peng, Y.B., Pan, T.M., Weng, W.H., Pang, S.T., Chi, L., 2013. International Journal of Electrochemcal Science 8, 606–620.
Hong, J., Xu, J., Gong, P., Yu, J., Ma, H., Yao, S., 2008. Microporous and Mesoporous Materials 109, 470–477.
Hood, J.D., Bednarski, M., Frausto, R., Guccione, S., Reisfeld, R.A., Xiang, R., Cheresh, D.A., 2002. Science 296, 2404–2407.
Hua, M.Y., Lin, Y.C., Tsai, R.Y., Chen, H.C., 2012. Journal of Materials Chemistry 22, 2566–2574.
Jeon, S., Hwang, H., 2002. Applied Physics Letters 81, 4856–4858.
Jeon, S., Hwang, H., 2003. Journal of Applied Physics 93, 6393–6395.
Katz, E., Willner, I., Wang, J., 2004. Electroanalysis 16, 19–44.
Lewin, M., Lewin, M., Carlesso, N., Tung, C.H., Tang, X.W., Cory, D., Scadden, D.T., Weissleder, R., 2000. Nature Biotechnology 18, 410–414.
Liao, C.W., Chou, J.C., Sun, T.P., Hsiung, S.K., Hsieh, J.H., 2007. Sensors and Actuators B 123, 720–726.
Lin, Y.H., Chiang, C.H., Wu, M.H., Pan, T.M., Luo, J.D., Chiou, C.C., 2011. Applied Physics Letters 99, 253704.
Matsuo, T., Esashi, M., Abe, H., 1979. IEEE Transactions on Electron Devices 26, 1856–1857.
Miao, Y., Guan, J., Chen, J., 2003. Biotechnology Advances 21, 527–534.
Pan, T.M., Liao, K.M., 2007. Sensors and Actuators B 128, 245–251.
Pan, T.M., Liao, K.M., 2008. IEEE Sensors Journal 8, 1856–1861.
Pan, T.M., Lin, J.C., Wu, M.H., Lai, C.S., 2009a. Sensors and Actuators B 138, 619–624.
Pan, T.M., Lee, C.D., Wu, M.H., 2009b. Journal of Physical Chemistry C 113, 21937–21940.
Pan, T.M., Lin, J.C., Wu, M.H., Lai, C.S., 2009c. Biosensors and Bioelectronics 24, 2864–2870.
Pan, T.M., Huang, M.D., Lin, C.W., Wu, M.H., 2010a. Sensors and Actuators B 144, 139–145.
Pan, T.M., Lin, C.W., Chiang, C.H., Huang, M.D., Chou, C.Y., 2010b. International Conference on Solid State Devices and Materials, Tokyo, Japan.
Pan, T.M., Liao, P.Y., Chang, K.Y., Lifeng, C., 2013. Electrochimica Acta 89, 798–806.
Perez, J.M., Simeone, F.J., Saeki, Y., Josephson, L., Weissleder, R., 2003. Journal of the American Chemical Society 125, 10192–10193.
Poghossian, A., Schoning, M.J., 2004. Electroanalysis 16, 1863–1872.
Rahimi, M., Wadajkar, A., Subramanian, K., Yousef, M., Cui, W., Hsieh, J.T., Nguyen, K. T., 2010. Nanomedicine 6, 672–680.
Schoning, M.J., Poghossian., A., 2006. Electroanalysis 18, 1893–1900.
van Dover, R.B., 1999. Applied Physics Letters 74, 3041–3043.
Veiseh, O., Gunn, J.W., Zhang, M., 2010. Advanced Drug Delivery Reviews 62, 284–304.
Wu, M.H., Lin, T.W., Huang, M.D., Wang, H.Y., Pan, T.M., 2010. Sensors and Actuators B 146, 342–348.
Wu, M.H., Lee, Y.F., Lin, C.W., Tsai, S.W., Wang, H.Y., Pan, T.M., 2011. Journal of Materials Chemistry 21, 539–547.
Yang, H.W., Hua, M.Y., Liu, H.L., Tsai, R.Y., Chuang, C.K., Chu, P.C., Wu, P.Y., Chang, Y. H., Chuang, H.C., Yu, K.J., Pang, S.T., 2012. ACS Nano 6, 1795–1805.